Cumulative reaction probabilities and transition state properties: A study of the $H^+ + H_2$ and $H^+ + D_2$ proton exchange reactions

P. G. Jambrina,[1,2] F. J. Aoiz,[2,a)] C. J. Eyles,[3] V. J. Herrero,[4,b)] and V. Sáez Rábanos[5,c)]
[1]*Departamento de Química Física, Universidad de Salamanca, 37008 Salamanca, Spain*
[2]*Departamento de Química Física, Facultad de Química, Universidad Complutense, 28040 Madrid, Spain*
[3]*Department of Chemistry, The Physical and Theoretical Chemistry Laboratory, University of Oxford, South Parks Road, Oxford OX1 3QZ, United Kingdom*
[4]*Instituto de Estructura de la Materia (CSIC), Serrano 123, 28006 Madrid, Spain*
[5]*Departamento de Química y Bioquímica, ETS Ingenieros de Montes, Universidad Politécnica, 28040 Madrid, Spain*

(Received 13 March 2009; accepted 15 April 2009; published online 8 May 2009)

Cumulative reaction probabilities (CRPs) have been calculated by accurate (converged, close coupling) quantum mechanical (QM), quasiclassical trajectory (QCT), and statistical QCT (SQCT) methods for the $H^+ + H_2$ and $H^+ + D_2$ reactions at collision energies up to 1.2 eV and total angular momentum $J=0-4$. A marked resonance structure is found in the QM CRP, most especially for the H_3^+ system and $J=0$. When the CRPs are resolved in their *ortho* and *para* contributions, a clear steplike structure is found associated with the opening of internal states of reactants and products. The comparison of the QCT results with those of the other methods evinces the occurrence of two transition states, one at the entrance and one at the exit. At low J values, except for the quantal resonance structure and the lack of quantization in the product channel, the agreement between QM and QCT is very good. The SQCT model, that reflects the steplike structure associated with the opening of initial and final states accurately, clearly tends to overestimate the value of the CRP as the collision energy increases. This effect seems more marked for the $H^+ + D_2$ isotopic variant. For sufficiently high J values, the growth of the centrifugal barrier leads to an increase in the threshold of the CRP. At these high J values the discrepancy between SQCT and QCT becomes larger and is magnified with growing collision energy. The total CRPs calculated with the QCT and SQCT methods allowed the determination of the rate constant for the $H^+ + D_2$ reaction. It was found that the rate, in agreement with experiment, decreases with temperature as expected for an endothermic reaction. In the range of temperatures between 200 and 500 K the differences between SQCT and QCT rate results are relatively minor. Although exact QM calculations are formidable for an exact determination of the $k(T)$, it can be reliably expected that their value will lie between those given by the dynamical and statistical trajectory methods. © *2009 American Institute of Physics*.
[DOI: 10.1063/1.3129343]

I. INTRODUCTION

Conventional transition state theory (TST) in chemical kinetics was originally developed for direct chemical reactions with a barrier.[1,2] The key assumption of the theory is the existence of a dividing surface at an intermediate configuration, which is crossed only once and limits the flux from reactants to products. In reactions leading to the formation of a long-lived complex, the potential energy surface (PES) has a well in the close interaction region, where the nuclei remain trapped and oscillate for a time. In this situation the definition of a dividing surface between reactants and products is not so straightforward and these systems are usually treated with statistical theories.[3,4] In the 1970s, Miller presented a unified statistical model[5] accounting for both direct and complex mechanisms which led in the direct and complex reaction extremes to the previously established TST and statistical theories and could also account for the intermediate cases between them. In this model the use of Keck's variational principle[6] provided a general criterion for the location of the relevant dividing surfaces, not only for reactive systems with saddle points or wells in their PES but also for more atypical situations such as "nonadiabatic trapping"[7,8] or orbiting complexes. For reactions with a potential energy well constrained by entrance and exit barriers, the relevant dividing surfaces (transition states) are close to the saddle points of the respective barriers. If the barriers, either dynamical or centrifugal, disappear the dividing surfaces shift to the asymptotic configurations of reactants and products.

In previous works the transition state properties of the $H+H_2$ and $F+H_2$ reactive systems have been analyzed in our group using the cumulative reaction probability (CRP) formalism[9,10] based on both quantum mechanical (QM) and quasiclassical trajectory (QCT) calculations.[11–13] The two mentioned systems are prototypes of direct reactions with a barrier, but have very different transition states. The TS of

[a)]Electronic mail: aoiz@quim.ucm.es.
[b)]Electronic mail: vherrero@iem.cfmac.csic.es.
[c)]Electronic mail: v.saez@upm.es.

$H+H_2$ is characterized by dynamical constraints derived from its high threshold and from its narrow and steep energetic valley in the vicinity of the collinear saddle point. In contrast, the transition state of the $F+H_2$ reaction, with a low early barrier and a shallow bending potential, imposes only a small energetic restriction, without an appreciable dynamical constraint to the reactivity. The different transition states are clearly imprinted in the shapes of the calculated CRPs.[11–13] In addition, a good global agreement was obtained between the quasiclassical and QM results.

Bearing in mind the conceptual framework of the unified statistical model of Miller,[5] which allows a natural extension of transition state notions to complex-forming reactions without saddle points in their potential surfaces, we have undertaken in this work an analysis of the relation between dynamics and transition state properties for the $H^+ + H_2$ reaction. The ground state PES for this reaction is barrierless and has a deep well ($\approx$4 eV) corresponding to H_3^+. This system, involving only two electrons, constitutes the simplest ion-molecule reaction and provides in principle a very good opportunity for the comparison between experiment and theory; in addition, its deuterated variants can play an important role in the deuterium fractionation observed in the interstellar medium;[14] as a consequence it has been intensively studied over the last decades (see, for instance, Refs. 15–37 and references therein). Much work was devoted to the role of nonadiabatic transitions between the various dynamic channels of the H_3^+ system,[15,27,29–31] but we will concentrate our attention in the proton (or deuteron) exchange process, which is the only reactive pathway open for collision energies below $\approx$1.6 eV. For this channel total cross sections and rate coefficients have been measured with different techniques.[17,21,22,24] Early theoretical studies using statistical models, limited trajectory calculations, and crude approximations for the PESs[16,19,20] could reproduce roughly the experimental data. These studies revealed also that both "complex-forming" and "direct-collision" mechanisms contribute to the reactivity, the former prevailing for the slower collisions and the latter increasing in importance with growing energy. Recently, accurate potential surfaces have been produced[29,33–35] and the quality of the dynamical calculations has increased greatly; extensive QCT calculations, refined statistical models, approximate and accurate (for a limited range of angular momenta) time independent QM treatments, as well as wave packet methods[27–32,36,37] have been now applied to the study of different aspects of the reaction considered, but the presence of the deep H_3^+ potential well still renders three dimensional, fully converged QM calculations difficult and very expensive.

In the present work we have performed calculations of CRPs for the proton exchange channel of the $H^+ + H_2$ and $H^+ + D_2$ reactions using three approaches: accurate QM, QCT, and the statistical QCT (SQCT) method.[36,37] The results are discussed paying special attention to the dynamical information derived from the comparison of the three theoretical approaches for the identification of the relevant transition states and of the dynamical limitations to the complex mechanism.

The article is structured as follows; Section II describes the various theoretical approaches and the details of the calculation; in Sec. III the results are presented and discussed. Finally, the most relevant conclusions are summarized in Sec. IV.

II. METHOD

The QM and QCT methods used in the present work for the calculation of CRPs have been described in previous articles.[11–13] Only the main details of these methods are briefly reviewed here. In addition the SQCT method previously developed for dynamical studies of insertion complex-forming reactions[36,37] is extended for the calculation of CRPs. All calculations were run on the PES of Aguado *et al.*[34]

A. QM CRPs

The reaction probability at a fixed total angular momentum quantum number J and total energy E for a specific rovibrational reagent's state v,j and initial helicity quantum number k, which corresponds to the projection of both **J** and **j** onto the initial relative velocity,[12,38] is given in terms of the scattering matrix, S, by

$$P_{vjk}^J(E) = \sum_{v',j',k'} |S_{v'j'k',vjk}^2|^2, \tag{1}$$

where the summation runs over all product's states, v', j' and $k' \in [-\min(J,j'), \min(J,j')]$, k' being the projection of **J** onto the final relative velocity, that are accessible at a given total energy. Note that a single arrangement for the products is implicitly assumed; if the number of possible product arrangements is larger the summation of Eq. (1) must also run over all product arrangements.

Summation in Eq. (1) over all the reagent quantum numbers leads to the definition of the "standard" CRP,

$$C_r^J(E) = \sum_{v,j,k} P_{vjk}^J(E). \tag{2}$$

The total CRP is usually defined as

$$C_r(E) = \sum_{J=0}^{J_{\max}} (2J+1) C_r^J(E), \tag{3}$$

where the sum over J extends up to the maximum value of the total angular momentum $J_{\max}$ leading to reaction.

The general expression of the thermal rate constant in terms of the total CRP is given by

$$k(T) = \frac{\int_0^\infty C_r(E) \exp(-E/k_B T) dE}{h \Phi_{\mathrm{rel}}(T) Z_{BC}(T)}, \tag{4}$$

where $\Phi_{\mathrm{rel}}(T)$ is the translational partition function for the relative motion,

$$\Phi_{\mathrm{rel}}(T) = \left(\frac{2\pi\mu k_B T}{h^2}\right)^{3/2}, \tag{5}$$

and $Z_{BC}(T)$ is the rovibrational partition function of the reagents.

In the case of a homonuclear molecule, the diatomic parity, $p=\pm$, has to be taken into account,

$$C_r^p(E) = \sum_J (2J+1) C_r^{J,p}(E) = \sum_J \sum_{v,j_p,k} (2J+1) P^J_{v j_p k}(E), \tag{6}$$

where j_p indicates even ($p=e$) and odd ($p=o$) rotational quantum numbers.

Specifically for the $H^+ + D_2$ reaction, the expression of the rate constant can be written as

$$k(T) = \frac{w^{(o)} \int_0^\infty C_r^{(o)}(E) \exp(-E/k_B T) dE + w^{(e)} \int_0^\infty C_r^{(e)}(E) \exp(-E/k_B T) dE}{h \Phi_{\mathrm{rel}}(T) Z_{\mathrm{D}_2}(T)}, \tag{7}$$

with

$$Z_{\mathrm{D}_2}(T) = w^{(o)} \sum_{v,j_o} (2j_o+1) e^{-\beta E_{v,j_o}} + w^{(e)} \sum_{v,j_e} (2j_e+1) e^{-\beta E_{v,j_e}}, \tag{8}$$

where $w^{(o)}=I(2I+1)$ and $w^{(e)}=(I+1)(2I+1)$ describe the nuclear spin weights for p-D_2 and o-D_2, respectively.

For the QM scattering calculations, the coupled-channel hyperspherical coordinate method of Skouteris *et al.*[38] has been used. Careful tests of convergence were made varying the maximum internal energy in any channel, $E_{\max}$, the maximum rotational quantum number $j_{\max}$, and the maximum hyperradius $\rho_{\max}$, trying to minimize the computational time. Converged CRPs were obtained using a basis set with diatomic energy levels up to $E_{\max}=4.3$ eV and $j_{\max}=60$. The value of $\rho_{\max}$ was $30a_0$, and 1000 log-derivative propagation sectors were used in the calculations. Using these parameters, it was found that the CRPs were converged to better than 0.5% for $J=0$, and that the resonance structures were exactly reproducible. For $J>0$, angular basis functions with helicities up to $k_{\max}$ were used, where $k_{\max}$ is the largest of $\min(J,j)$ or $\min(J,j')$. This amounted to 4731 channels (o-D_2), 4713 (p-D_2) for HD_2^+, and 2950 channels for H_3^+ at $J=4$. A total of 400 total energies between 0.2336 and 1.2 eV have been calculated for the HD_2^+ system at $J=0$ and $J=1$, and 940 and 210 total energies for the $H^+ + p$-H_2 and HD_2^+ systems, respectively, at $J=4$. Note that both diatomic parities for each reaction have been calculated.

B. Quasiclassical CRPs

The QCT method to determine the CRP has been described in detail in previous publications.[11,12] For each combination of (J,j) quantum (integer) numbers, the helicity quantum number k is chosen by uniform sampling with integer values in the $-\min(J,j) \leqslant k \leqslant \min(J,j)$ interval. With this sampling the quasiclassical counterpart of Eq. (1) is given by

$$P^J_{vjk}(E) = \frac{N_r(E,J;v,j,k)}{N(E,J;v,j,k)}, \tag{9}$$

where N_r is the number of reactive trajectories and N the total number of trajectories run under the given set of initial conditions (specified by the values of E, J, v, j, and k).

Once this quantity is determined, the QCT CRPs and the thermal rate constant are calculated through the use of Eqs. (2), (6), and (7).

In the present work the QCT CRP dependent on J and the total CRP has been calculated by sampling the total energy randomly and uniformly within the energy interval considered. Once the value of E is fixed for each trajectory, the total number of energetically accessible states, $n(E)$, is determined and the initial v, j state is randomly selected with equal probability from that set of states. The rest of initial conditions are selected as in Ref. 12. Then the CRP as a function of E can be fitted to a series of Legendre polynomials as detailed in Ref. 11. Using this sampling, the rate constants can be calculated directly without needing to determine the total CRP and avoiding the numerical integration as shown in Ref. 11.

To overcome the problem of the zero point energy of the products in the calculation of the rate constant, where it has an important repercussion, the Gaussian binning method[39–42] was applied to the calculation of the total CRP and rate constants.

The QCT calculations were done by running batches of 1×10^6 trajectories at variable total energy and fixed J (3×10^6 trajectories at $J=4$). To determine the total CRP and $k(T)$ for the $H^+ + D_2$ reaction, 2.5×10^6 trajectories were run at variable total energy and variable J. Trajectories were started at an initial distance $R_0=10$ Å, and an integration time step of 0.04 fs ensured an energy conservation better than 1 in 10^5. The initial rovibrational energies were calculated semiclassically using the asymptotic diatomic potential energy of the PES; they agree with their exact, quantum counterparts to within four significant figures.

C. SQCT

The statistical model assumes that all reactive collisions proceed via formation of a collision complex whose lifetime is long enough as to treat its formation and decay as independent events. Under these assumptions, the reaction probability at a given total energy E, total angular momentum J, and a triatomic parity P $(=\pm 1)$ from a given reagent state characterized by v, j, and k, vibrational, rotational, and helicity quantum numbers, respectively, to a final state of the products given by v', j', and k' can be written as[43,44]

$$P^{J,P}_{v'j'k'vjk}(E) = p^{J,P,\alpha}_{vjk} \times \frac{p^{J,P,\alpha'}_{v'j'k'}}{D^{J,P}}, \tag{10}$$

where $p^{J,P,\alpha}_{vjk}$ and $p^{J,P,\alpha'}_{v'j'k'}$ are, respectively, the capture probabilities (the probabilities of forming the collision complex) from the reagent arrangement channel α and from the product arrangement channel α'. The quotient of Eq. (10) represents the fraction of collision complexes that decay into the product channel v',j',k'. The capture probability for each channel is given by

$$p^{J,\alpha}_{vjk} = \frac{N^{\alpha}_{c}(J,v,j,k)}{N^{\alpha}(J,v,j,k)}. \tag{11}$$

Here $N^{\alpha}(J,v,j,k)$ and $N^{\alpha}_{c}(J,v,j,k)$ are, respectively, the total number of trajectories and the number of these captured for given values of J,v,j,k in the arrangement channel α. The values of k are restricted to integers in the interval $k \in [0,k_{\max}]$, where $k_{\max}=\min(J,j)$; that is, only the absolute value of k is considered. The triatomic parity P is introduced as in the QM treatment.[44] Of the two possible triatomic parities, $P=(-1)^J$ and $P=(-1)^{J+1}$, $k=0$ only contributes to the former, whereas the $k>0$ values appear in both parities; i.e.:

$$p^{J,P,\alpha}_{vjk} = p^{J,\alpha}_{vjk} \quad \text{for } P=(-1)^J, \quad (-1)^{J+1} \quad \text{when } k \neq 0,$$

$$p^{J,P,\alpha}_{vjk} = p^{J,\alpha}_{vjk}\delta_{P,(-1)^J} \quad \text{when } k=0. \tag{12}$$

In the case of three distinguishable arrangement channels, the denominator, $D^{J,P}$, of Eq. (10) is given by

$$D^{J,P} = \sum_{\alpha''=1}^{3} \sum_{v''j''k''} p^{J,P\alpha''}_{v''j''k''} = \sum_{\alpha''=1}^{3} \sum_{v''j''} Q^{J,P\alpha''}_{v''j''}, \tag{13}$$

that is, the sum of capture probabilities over all arrangements and all possible states accessible at a total energy E.[36,37]

In the case of homonuclear molecules, the diatomic parity, $p=o/e$, has to be taken into account. In this case the reaction probability summed over all final states must be written as[44]

$$P^{J}_{vj_pk}(E) = \sum_{P} p^{J,P\alpha}_{vj_pk} \times \sum_{v',j'} \frac{Q^{J,P\alpha'}_{v'j'}}{D^{J,P,p}}, \tag{14}$$

where $D^{J,P,p}$ is given by

$$D^{J,P,p} = \sum_{v,j_p} Q^{J,P\alpha}_{vj_p} + \sum_{v',j'} Q^{J,P\alpha'}_{v'j'}. \tag{15}$$

The first sum only runs over odd or even rotational states depending on the diatomic parity.

The SQCT (or SQM) diatomic parity dependent CRP can be written as

$$C^{J,p}_{r}(E) = \sum_{P} \sum_{v,j_p} Q^{J,P\alpha}_{vj_p} \times \frac{\Sigma_{v',j'} Q^{J,P\alpha'}_{v'j'}}{D^{J,P,p}}, \tag{16}$$

that is, the sum over all initial states of the $P^{J}_{vj_pk}(E)$ reaction probabilities.

Analogously to the QCT method, to calculate the energy dependent $C^{J,p}_{r}(E)$ it is advantageous to sample the total energy randomly and uniformly within a preselected $[E_1,E_2]$ interval. Once the energy has been selected, the total number of energetically open states of the diatom, $n(E)$, is determined and the initial rovibrational (v,j) state is randomly selected from that set of accessible states. In a next stage, the helicity quantum number is also randomly selected in the above mentioned interval leading to the initial conditions for each trajectory.

When the energy is continuously scanned, the sum of capture probabilities of a given triatomic and diatomic parities for reagents, $\Sigma_{v,j_p} Q^{J,P\alpha}_{v,j_p}$, the sum of capture probabilities over all accessible product's states, $\Sigma_{v',j'} Q^{J,P\alpha'}_{v'j'}$, and the denominator $D^{J,P,p}$ of Eq. (16) [each of them generically labeled $\Gamma(E)$] have been expanded in terms of a series of Legendre polynomials[11] as

$$\Gamma(E) = \frac{2Q}{E_2 - E_1} \sum_{m=0}^{M} a_m P_m[x(E)], \tag{17}$$

where $P_m(x)$ is the mth degree Legendre polynomial whose argument is the reduced variable $x(E)$ defined in $[-1,1]$,

$$x(E) = \frac{2E - E_2 - E_1}{E_2 - E_1}. \tag{18}$$

The normalization constant Q in Eq. (17) is given by

$$Q = \frac{W_{\text{tot}}}{N(J)}(E_2 - E_1), \tag{19}$$

where $N(J)$ is the total number of trajectories, captured or not, relevant for each of the quantities above mentioned, and W_{tot} is the sum of the weights w_i of each individual captured trajectory, i.e.,

$$W_{\text{tot}} = \sum_{i=1}^{N_c} w_i, \tag{20}$$

$$w_i = [2\min(J_i,j_i)+1]n(E_i), \tag{21}$$

where E_i, J_i, and j_i are the total energy, the total and

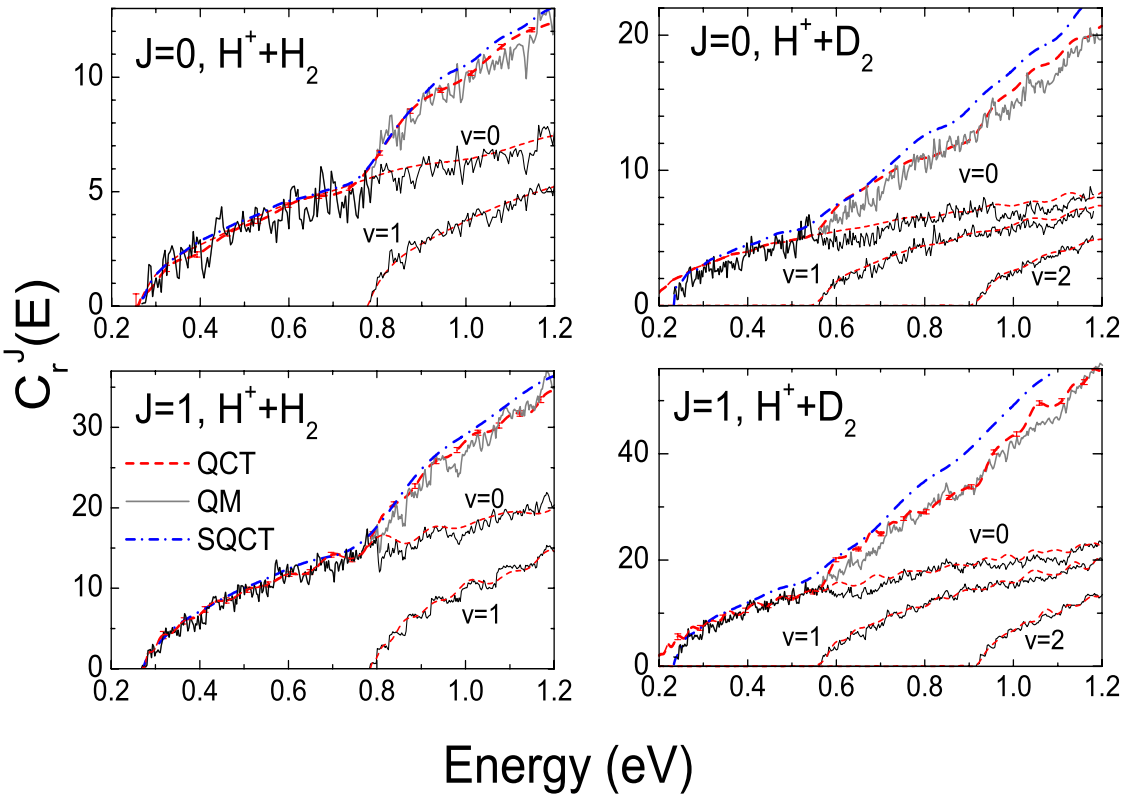

FIG. 1. (Color online) QM (solid line, black), QCT (dashed line, red), and SQCT (dash dot, blue) CRPs as a function of the total energy for the $H^+ + H_2$ (left panels) and $H^+ + D_2$ (right panels) for $J=0$ (top) and $J=1$ (bottom). In each case the contributions from the initial vibrational states ($v=0,1$ for $H^+ + H_2$ and $v=0,1,2$ for $H^+ + D_2$) are also represented. The CRPs are the unweighted sums of the *ortho* and *para* contributions.

rotational angular momentum quantum numbers, respectively, for the ith captured trajectory, and $n(E_i)$ is the total number of energetically accessible states at E_i. The sum runs over the relevant subset of captured trajectories, N_c.

Once these $\Gamma(E)$ functions are calculated, they are combined in Eq. (16) to obtain the corresponding $C_r^{J,p}(E)$. The method was tested by comparison with the CRP obtained at a fixed energy (see Sec. III).

To determine the total CRP one should use the CRP for each individual J value as a function of energy or, alternatively, by calculating the total CRP for each individual energy and diatomic parity using in both cases, Eqs. (16) and (6), which has been the procedure used in the present work.

The rate constants $k(T)$ have been determined using Eq. (7) interpolating the product of the Boltzmann factor and the total CRP; that is, the thermal total CRP, using a spline routine.

As in previous works,[36,37] the criterion of capture to establish that a given trajectory has surmounted the centrifugal barrier giving rise to the formation of a collision complex was based on the value of the potential energy. If the trajectory reached a value of $V_{cap}=-0.6$ eV, it was considered as a trapped trajectory.

Batches of 10^6 trajectories have been run for each arrangement channel at variable collision energies and fixed value of J. To determine the total CRP, calculations were carried out at 20 total energies from 0.234 eV (the threshold for HD formation) to 1.6 eV running 3×10^5 trajectories per energy and channel. The initial integration distance and time integration step were as in the QCT calculations.

III. RESULTS AND DISCUSSION

Figure 1 shows QCT, SQM, and QM $C_r^J(E)$ for the $H^+ + H_2$ and $H^+ + D_2$ reactions at $J=0,1$. The CRPs shown in this figure are the sum of the even (*para* for H_2 and *ortho* for D_2) and odd (*ortho* for H_2 and *para* for D_2) j contributions neglecting the nuclear spin statistics. In any case, the even and odd initial j contributions to the total CRP are practically the same, except for some fine structure due to the existing resonance structures. The decomposition of $C_r^J(E)$ for reaction with H_2 and D_2 molecules excited to their initial vibrational levels is also shown. The successive opening of these initial vibrational levels is reflected in the smooth steplike structure observable in the global $C_r^J(E)$.

All the CRPs increase monotonically with total energy with noticeable rises when the initial vibrational states become open. Except for the fast oscillations corresponding to the resonance structure in the QM CRPs, the agreement between the three methods is very good for the $H^+ + H_2$ isotopic variant. For $H^+ + D_2$ the SQCT CRPs become clearly larger than those from the other two methods with growing energy. The resonance oscillations are more marked for the reaction with the lighter H_2 molecules and for $J=0$.

CRPs for the $D^+ + H_2$ deuteron exchange process at $J=0$ have been calculated by Takayanagi *et al.*[27] on a diatomics-in-molecule surface using both a simple statistical model (simply counting initial and final states) and a close-coupling QM method. The QM $C_r^{J=0}(E)$ are similar in shape to those of the present work exhibiting a step structure with superimposed resonance oscillations. The very good agree-

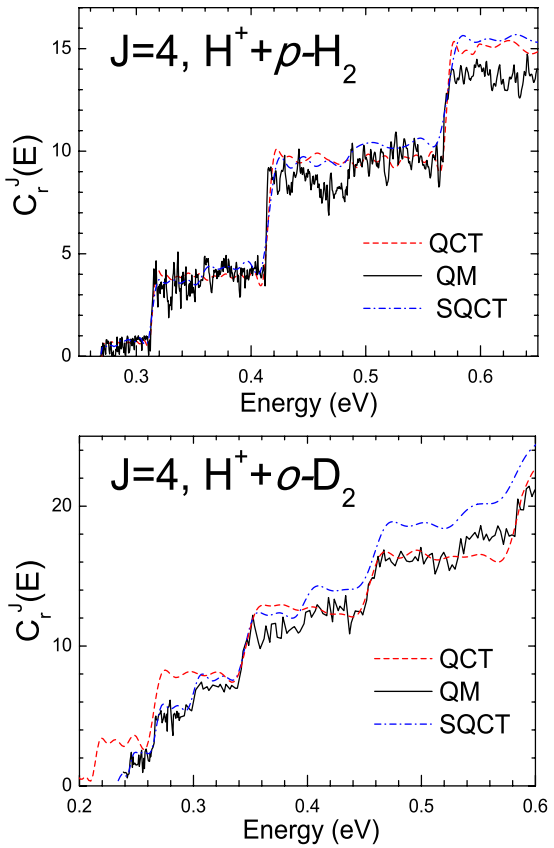

FIG. 2. (Color online) CRPs as a function of the total energy for the $H^+ + p\text{-}H_2$ reaction (upper panel) and for the $H^+ + o\text{-}D_2$ reaction (lower panel). The calculations correspond to a total angular momentum $J=4$. Solid line (black): QM results. Dashed line (red): QCT results. Dot-dashed line (blue): SQCT results.

ment found by these authors between statistical and QM results until an energy of 2.0 eV indicates that for $J=0$ the reaction proceeds essentially through a complex mechanism. However, in the present case, the results of Fig. 1 seem to indicate that the extent of the statistical character of the reaction mechanism depends on the isotopic variant considered. In particular, a clear deviation between statistical and dynamical calculations is found for $H^+ + D_2$ in contrast with the results for the $D^+ + H_2$ reaction, and to a less extent with those for the $H^+ + H_2$ system. Calculations have been also carried out counting states of the reagent and product channels assuming that the capture probabilities are equal to 1 for all the open states. As expected, the agreement between the SQCT and this simple procedure is very good for low J values for which the centrifugal barrier is practically negligible.

The steplike structure in the $C_r^J(E)$ is best seen for reactions at low energy (i.e., before the opening of the $v=1$ and/or $v'=1$), for higher J, and for the *ortho* and *para* variants of the molecular species that have rotational levels separated by two quanta. This is clearly shown in Fig. 2 where QCT, SQCT, and QM CRPs for $J=4$ are represented for the reactions of $H^+ + p\text{-}H_2$ (upper panel) and $H^+ + o\text{-}D_2$ (lower panel). The larger spacing between the rotational levels of the H_2 molecule is reflected in the wider steps of its $C_r^{J=4}(E)$ as compared with those of D_2. The steps in the $C_r^{J=4}(E)$ of Fig. 2 are higher than those in $C_r^{J=0}(E)$ in Fig. 1 due to the larger number of helicity (k) states associated with the higher value of the angular momentum. In the case of $J=0$ the only helicity value allowed, which is $\min(J,j)$, is $k=0$. For $J=4$ the number of possible k states increases with the opening of successive j up to $k=4$; for $j=0$ only one value ($k=0$) is possible (note the small steps at the threshold of the CRPs in Fig. 2); for $j=2$, five k states ranging from $k=-2$ to $k=+2$ in integer steps are allowed; analogously for $j=4$ there are nine k states allowed. Beyond this j value, there are no further increases in the step height since the maximum number of k states remains limited by the value of J (see Ref. 13 for a discussion on the effect of helicity in the shape of the CRPs for $F + H_2$).

The fast resonance oscillations in the QM results superimposed on the steps of the $C_r^J(E)$ for $J=4$ are also clearly visible. The good coincidence of the step location with the opening of the successive rotational states of $p\text{-}H_2$ is indicative of an unconstrained transition state early in the entrance channel and determined just by the accessibility of the different internal states of the molecule at a given energy. Both $o\text{-}H_2$ and $p\text{-}H_2$ molecules are produced through the $H + p\text{-}H_2$ reaction. The structure of odd states of H_2 is also imprinted in the CRP, but this structure is not so evident in the upper panel of Fig. 2. Within the statistical model used in the present work, the contribution to $C_r^{J,p}(E)$ from the various open rovibrational states of the reactants v,j and products v',j' can be easily calculated from Eq. (16). Application of this equation to the conditions of Fig. 2 leads to a sharp increase in $C_r^{J=4}(E)$ for the opening of the successive rotational states of the reactants, which determine the steplike structure, and to a much smaller increase for the opening of the rotational states of the products. In fact, the production of H_2 in odd levels can be found upon close inspection of the figure, in the form of a small rise in the middle of the wide steps calculated with the QM and SQCT methods. The QCT calculations do not include a quantization in the exit channel, therefore the step rise only takes place when the reactant states are open.

The considerations of the previous paragraph do not take into account the influence of the conservation of nuclear spin and diatomic parity for the outcome of this reaction, which was highlighted in previous studies[45–47] stressing that *ortho*- to *para*-hydrogen conversion has a very low probability due to unfavorable statistics.

The agreement between the three theoretical methods is, in general, good in the case of $p\text{-}H_2$, but there are appreciable discrepancies for the $H^+ + o\text{-}D_2$ reaction, both at the low and high ends of the energy range considered. At low energies the QCT $C_r^J(E)$, which contemplates only the quantization of the entrance channel, has less steps and is clearly different from those of the other two methods. The SQCT and QM approaches take into account the quantization of the molecular energy levels for reactants and products. In the QCT CRP the threshold is lower, since reaction is possible for energies just beyond that of the ground rovibrational level of D_2 (0.19 eV), and the appearance of the steps in the $C_r^J(E)$ corresponds roughly to the energies of the successive rotational levels of $o\text{-}D_2$ (i.e., $j=0,2,4\ldots$). The SQCT and

QM CRPs have higher thresholds because the energy of the ground rotational level of HD (0.23 eV) must be reached for reaction to take place. The steps in the SQCT and QM $C_r^J(E)$ correspond to the opening of rotational channels of either o-D_2 (even levels of D_2) or HD (odd and even levels). The comparison of the QCT results with those of the other two methods evinces in a clear way the occurrence of two transition states, one at the entrance and one at the exit, for the reaction considered. The steps coincident in the three methods correspond to the transition state of the entrance channel, whereas those absent in the QCT results mark the transition state of the exit channel. The lower panel of Fig. 2 illustrates in a clear way the picture provided in the unified statistical model of Miller[5] reflecting that in the absence of entrance or exit barriers the transition states (reaction bottlenecks) tend asymptotically toward the respective reactant's and product's configurations.

We can now compare this result with the information about the transition state of the direct $H+H_2$ and $F+H_2$ reactions obtained with the same CRP formalism in previous works.[11–13] The marked steplike structure in the cumulative reactive probabilities displayed in Fig. 2 is in contrast with the much smoother evolution obtained for the dynamically constrained $H+H_2$ reaction.[11,12] In this case the reaction path follows a narrow energetic valley with a high barrier, which has a minimum for a collinear nuclear configuration. The corresponding CRP reflects not only the opening of the successive internal states but also the strong and dominating dependence of the barrier on the angle of attack, which is a continuous function and tends to blur the structure. The CRP of the $F+H_2$ reaction,[13] which has only a very small barrier and a very broad bending potential, has a step structure similar to that of $H^+ + H_2$, but with one important difference: in the reaction with fluorine atoms there is just one transition state, at the location of the low early barrier and the steps in the CPR reflect just the internal level structure of the H_2 molecule. The reaction is exoergic and once the barrier is surmounted, the reaction takes place with unit probability, and the exit channel imposes no further restrictions to the reactivity due to the very high number of product's states available. Consequently, the QM calculations do not produce a double step structure in the CRP like that shown in the lower panel of Fig. 2.

Going back to the lower panel of Fig. 2 one can observe that with growing energy the QM and QCT CRPs become similar, but for energy values beyond 0.4 eV, the SQCT $C_r^J(E)$ starts to deviate from the other two, following the trend already shown for this isotopic variant in Fig. 1. In Fig. 3, the CRPs for the reactions of H^+ with *ortho* and *para* D_2 are represented over an enlarged energy range reaching to 1 eV. The SQCT CRP becomes gradually larger than the other two, which remain in very good agreement up to 1 eV, except for the marked QCT step at about 0.7 eV in the $H^+ + p$-D_2 reaction. This step is due to the simultaneous opening of the $v=0$, $j=11$ and $v=1$, $j=5$ rovibrational levels of p-D_2. In the QM calculation this step is smoothed by the presence of energy levels of HD between those of p-D_2 that limit the reactivity in the exit channel and prevent the abrupt rise observed in the QCT. The divergence between the statistical

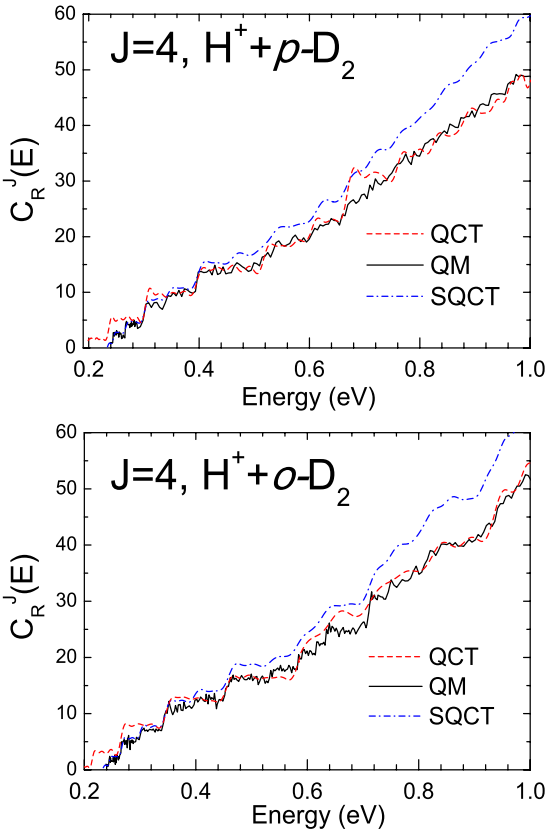

FIG. 3. (Color online) CRPs as a function of the total energy for the $H^+ + p$-D_2 (upper panel) and $H^+ + o$-D_2 (lower panel) over the 0.19–1.0 eV total energy range and for $J=4$. Lines (and colors) as in Fig. 2.

and the purely dynamical CRP is indicative of the growing contribution of more direct collisions which do not proceed to the formation of products. Note that the mentioned divergence in the $C_r^{J=4}(E)$ takes place for energies beyond approximately 0.4 eV.

The difference between statistical and dynamical results grows also with increasing J as illustrated in Fig. 4 where the QCT and SQCT CRP for $H^+ + D_2$ is shown for $J=20$ and $J=40$. Accurate QM calculations for the large angular momenta considered here would be extremely expensive computationally and have not been performed. For these high J values and without resolution in *ortho* and *para* states of the reactants, the steplike structure is practically smoothed out. The increase in J from 20 to 40 leads to an increase in the threshold due to the growth of the centrifugal barrier and to a decrease in the value of both the SQCT and QCT CRPs, but the decrease is much more marked in the case of the QCT calculations. Notice also that the total energy thresholds of QCT and SQCT calculations ($\approx$0.25 eV for $J=20$ and 0.48 eV for $J=40$) are almost coincident, in contrast to that observed at low J values, reflecting the fact that the transition state is no longer at asymptotic distances but at the location of the broad centrifugal barrier. The appearance of reaction is thus dominated by this barrier and not by the energetic accessibility of initial or final states. This is also underpinned by simple statistical calculations counting the number of states. As J increases, the CRPs predicted by this method become progressively larger than those obtained with the

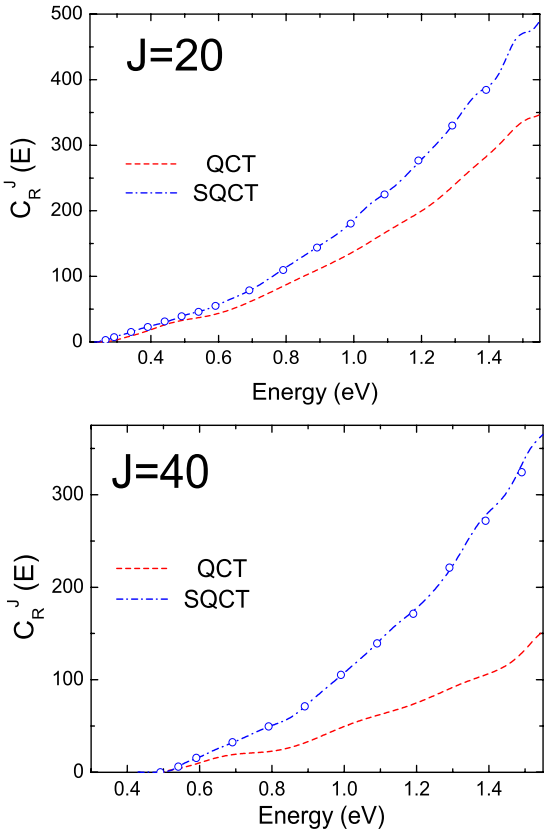

FIG. 4. (Color online) CRPs as a function of the total energy for the $H^+ + D_2$ reaction for $J=20$ (upper panel) and for $J=40$ (lower panel). Dashed line (red), QCT results; dot-dashed (blue) line, SQCT results calculated varying continuously the collision energy. Open circles, SQCT CRPs calculated at each individual collision energy (see Sec. II C), showing the coincidence between these two calculations. The CRPs are the unweighted sums of the *ortho* and *para* contributions.

SQCT since the method based on counting states neglects the centrifugal barrier.

Finally, in Fig. 5 the SQCT and QCT dynamical calculations of the total CRP including all J values weighted by $2J+1$ are presented. In spite of the logarithmic scale used in this plot, the growth of the total CRP with energy is faster than that for particular J values discussed thus far and the discrepancy between statistical and dynamical QCT calculations persists. Notice that the total CRP calculated with the QCT method incorporates the Gaussian binning treatment

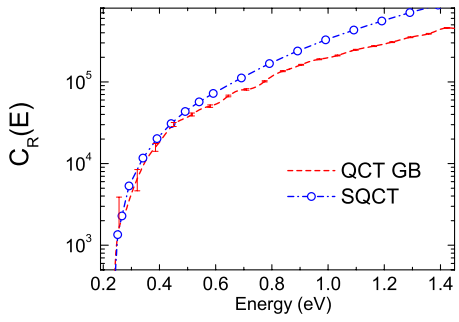

FIG. 5. (Color online) Total CRP as a function of the total energy summing the *ortho* and *para* contributions, as in Eq. (3), for the $H^+ + D_2$ reaction. Dashed line: QCT result calculated using the Gaussian binning method. Dot-dashed line with symbols: SQCT result.

and therefore the results are coincident with those from the SQCT calculations at the lowest energies near the reaction threshold.

In the previous paragraphs we have shown that both growing energy and growing angular momentum lead to a deviation between statistical and dynamical results. The most likely explanation for this behavior is a progressive loss of ergodicity; i.e., an inability to randomize the energy in the complex.[48] Dumont and Brumer[49] demonstrated that the existence of a relaxation time different from zero would introduce a nonstatistical component in the unimolecular lifetime distribution of a complex. From a comparison of Rice–Rampsperger–Kassel–Marcus and trajectory calculations in the H_3^+ complex, Berbinger and Schlier[48] estimated that the induction time needed to form a statistical complex in this system, for the range of energy and angular momentum of the present work, would be of the order of 50 fs. Trajectories dwelling for shorter times in the potential well of the complex (direct trajectories) will contribute to a nonstatistical behavior. The gradual increase in the proportion of direct trajectories with growing energy was already pointed out in the pioneering dynamical studies on this system, carried out with approximate potential surfaces and a limited number of trajectories.[19,20] The present, more rigorous calculations on a new *ab initio* PES corroborate this result and show that the deviation from the statistical model is due to the fact that collisions that reach the well are dynamically rebounded into the reactant channel. The role of angular momentum is more complicated to grasp intuitively. For a given energy, a moderate decrease with growing J is observed in the SQCT CRP (compare the two panels of Fig. 4). This effect can be traced back to the growth of the centrifugal barrier, related to the long range attractive potential, which is located at an appreciable distance from the region of strong interaction, outside the capture radius used in the SQCT model. The much larger decrease in the QCT CRP with angular momentum shown in the same figure has to do with the appearance of an effective repulsive potential associated with a centrifugal motion within the deep triatomic well of the complex. This repulsion takes place beyond the assumed capture radius and thus cannot be accounted for by the statistical model.

Using the QCT and SQCT $C_r(E)$, the thermal rate coefficient $k(T)$ for this reaction can be derived in a straightforward manner.[11] In Fig. 6, the calculated rate coefficients are shown and compared to the "most dynamically biased" (MDB) statistical model calculations of Gerlich[14,20] and to the experimental values measured with two techniques: flowing afterglow[18] and selected ion flow tube (SIFT).[21] The results from the two statistical models (MDB and SQCT) are very similar and diverge from the QCT rate constants with growing temperature. At ≈200 K the MDB and SQCT values are in very good agreement with the SIFT measurement.[21] The QCT rate coefficient is somewhat smaller, but lies within the experimental uncertainty of the SIFT and flowing afterglow experimental values.[18,21] At ≈300 K the results of the three calculations lie within the large error bar of the flowing afterglow measurement, but the QCT rate constant is in good agreement with the more precise SIFT result, whereas the statistical model rate constants

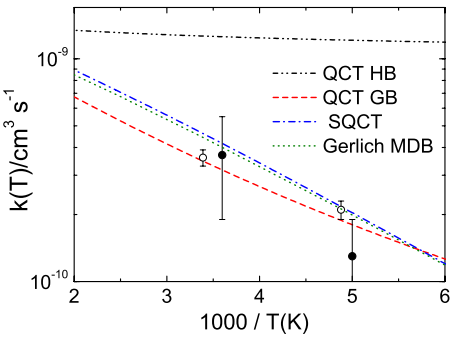

FIG. 6. (Color online) Thermal rate coefficient $k(T)$ for the $H^+ + D_2$. Dashed (red) line: QCT result with Gaussian binning. Dash-dot-dot-line (black) QCT with histogrammatic binning (see text). Dot-dashed (blue) line SQCT result. Short-dotted line (dark green): MDB statistical model results (Refs. 14 and 20). Closed symbols: Flowing afterglow measurements (Ref. 18). Open symbols: SIFT measurements (Ref. 21).

are larger. The results of the three theoretical approaches are also consistent with the upper limit of 5×10^{-11} cm^3 s^{-1} reported by Fehsenfeld *et al.*[18] for the rate coefficient at 80 K. The crucial role of the difference between the HD and D_2 zero energy levels (i.e., the difference of the zero point energies that causes the endoergicity threshold) for the reactivity of the system is also illustrated in the figure. The upper line in Fig. 6 corresponds to the result of a QCT calculation using the traditional histogrammatic binning for the assignment of reactive trajectories instead of the Gaussian binning procedure employed for the calculation of the total CRP and $k(T)$ (dashed line). The histogrammatic binning obviates the existence of the threshold by counting as reactive all trajectories leading to HD, even if the energy lies below the zero point energy of the molecule. As can be seen, removing the energetic threshold leads to an appreciable larger rate coefficient ($>1 \times 10^9$ cm^3 s^{-1}), weakly depending on temperature, as expected for a truly barrierless exoergic or thermoneutral reaction.

IV. SUMMARY AND CONCLUSIONS

The CRP formalism has been used for the investigation of the H_3^+ reactive system. In previous works, a quasiclassical method to obtain the CRPs has been developed, and the results have been compared with those calculated by exact QM methods for direct-type reactions such as $H + H_2$ and $F + H_2$ systems. In this article the statistical quasiclassical method has been implemented to calculate the CRPs. The three versions (QM, quasiclassical, and statistical quasiclassical) have been applied to the study of the complex-forming $H^+ + H_2$ and $H^+ + D_2$ proton exchange reactions whose potential surface has a deep well between reactants and products. The calculation of CRPs with the three approaches evinces the structure of the transition states for these reactions and provides valuable dynamical information. The CRPs for specific values of the total angular momentum exhibit a step structure characteristic of a transition state without dynamical constraints.

The analysis of the step structure shows that the reactions have two transition states (dynamical bottlenecks), one at the entrance, determined by the accessibility of successive internal states of the reactants, and one at the exit due to the internal states of the products. This can be clearly illustrated by running the quasiclassical trajectories, without quantization in the exit channel and comparing the result with that of the other two methods where product quantization is included. The effect can be better appreciated in the asymmetric $H^+ + o\text{-}D_2 \rightarrow HD + D^+$ reaction, with different spacings in the internal states of reactants and products. Although the same effect can also be observed in the $H^+ + p\text{-}H_2 \rightarrow H^+ + H_2$, which produces $o\text{-}H_2$ and $p\text{-}H_2$, the CRP steps associated with the product molecules are less appreciable in comparison with the steps corresponding to the reactant $p\text{-}H_2$. In this case, the resulting CRP reflects basically the structure of the entrance channel.

With increasing energy and angular momentum, the CRP calculated with the statistical method becomes substantially larger than those from the QCT and QM approaches. In accordance with previous works by other groups, the discrepancy with growing energy is attributed to an incomplete randomization of the initial energy with decreasing interaction time, which is not accounted for by the statistical models. The resulting more direct interactions favor a return of the system to the reactants channel. The divergence with growing J is due to a short range centrifugal repulsion taking place inside the deep triatomic well in the potential surface of H_3^+, also not considered in the statistical model, which assumes a capture radius outside the well.

SQCT and QCT thermal rate coefficients were derived for $H^+ + D_2$ from the corresponding CRPs converged in J. QM rate constants were not calculated because QM convergence in J is very costly for this reaction with a deep attractive well. The SQCT and QCT rate coefficients grow with increasing temperature, but the SQCT $k(T)$ grows faster. The SQCT $k(T)$ is found to be in good accordance with the result of a previous dynamically biased statistical model developed for an approximate potential surface using a limited number of trajectories. A comparison with experimental measurements shows a good global agreement, which is somewhat better for the QCT calculations than for statistical models at higher temperatures ($T \approx 300$ K).

ACKNOWLEDGMENTS

This work has been funded by the MICIN (Spain) under Project Nos. CTQ2008-02578, CTQ2005-09185, FIS2007-62006 ENE2006-14577-C04-Co3/FTN, and FIS2007-61686. P.G.J. also acknowledge support from the fellowship Grant No. Grant AP2006-03740. The research was conducted within the Unidad Asociada Química Física Molecular between the UCM and the CSIC of Spain.

[1] H. Eyring, J. Chem. Phys. **3**, 107 (1935).
[2] M. G. Evans and M. Polanyi, Trans. Faraday Soc. **31**, 875 (1935).
[3] J. C. Light, Discuss. Faraday Soc. **44**, 14 (1967).
[4] E. E. Nikitin, *Theory of Elementary Atomic and Molecular Processes in Gases* (Oxford University Press, New York, 1974).
[5] W. H. Miller, J. Chem. Phys. **65**, 2216 (1976).
[6] J. C. Keck, Adv. Chem. Phys. **13**, 85 (1967).
[7] S. F. Wu and R. D. Levine, Mol. Phys. **22**, 881 (1971).
[8] E. Pollak and P. Pechukas, J. Chem. Phys. **70**, 325 (1979).
[9] W. H. Miller, J. Chem. Phys. **61**, 1823 (1974).
[10] W. H. Miller, Acc. Chem. Res. **9**, 306 (1976).

[11] F. J. Aoiz, M. Brouard, C. Eyles, J. F. Castillo, and V. Sáez Rábanos, J. Chem. Phys. **125**, 144105 (2006).
[12] F. J. Aoiz, V. J. Herrero, M. P. de Miranda, and V. Sáez Rábanos, Phys. Chem. Chem. Phys. **9**, 5367 (2007).
[13] F. J. Aoiz, V. J. Herrero, and V. Sáez Rábanos, J. Chem. Phys. **129**, 024305 (2008).
[14] D. Gerlich and S. Schlemmer, Planet. Space Sci. **50**, 1287 (2002).
[15] J. C. Tully and K. Preston, J. Chem. Phys. **55**, 562 (1971).
[16] J. R. Krenos, R. K. Preston, R. Wolfgang, and J. C. Tully, J. Chem. Phys. **60**, 1634 (1974).
[17] G. Ochs and E. Telloy, J. Chem. Phys. **61**, 4930 (1974).
[18] F. C. Fehsenfeld, D. L. Albritton, Y. A. Bush, P. G. Fournier, T. R. Govers, and J. Fournier, J. Chem. Phys. **61**, 2150 (1974).
[19] D. Gerlich, U. Nowotny, Ch. Schlier, and E. Teloy, Chem. Phys. **47**, 245 (1980).
[20] D. Gerlich, in Symposium on Atomic and surface Physics, edited by W. Lindinger, F. Howorka, T. D. Mark, and F. Egger, Institut für Atomphysik der Universität Innsbruck, 1982), p. 304.
[21] M. J. Henchman, N. G. Adams, and D. Smith, J. Chem. Phys. **75**, 1201 (1981).
[22] H. Villinger, M. J. Henchman, and W. Lindinger, J. Chem. Phys. **76**, 1590 (1982).
[23] Ch. Schlier, U. Novotny, and E. Teloy, Chem. Phys. **111**, 401 (1987).
[24] D. Gerlich, Adv. Chem. Phys. **82**, 1 (1992).
[25] S. Chapman, Adv. Chem. Phys. **82**, 423 (1992).
[26] A. Ichihara, T. Shirai, and K. Yokoyama, J. Chem. Phys. **105**, 1857 (1996).
[27] T. Takayanagi, Y. Kurosaki, and A. Ichihara, J. Chem. Phys. **112**, 2615 (2000).
[28] T. González-Lezana, A. Aguado, M. Paniagua, and O. Roncero, J. Chem. Phys. **123**, 194309 (2005).
[29] H. Kamisaka, W. Bian, K. Nobusada, and H. Nakamura, J. Chem. Phys. **116**, 654 (2002).
[30] T. S. Chu and K. L. Han, J. Phys. Chem. A **109**, 2050 (2005).
[31] R. F. Lu, T. S. Chu, and K. L. Han, J. Phys. Chem. A **109**, 6683 (2005).
[32] E. Carmona-Novillo, T. González-Lezana, O. Roncero, P. Honvault, J. M. Launay, N. Bulut, F. J. Aoiz, L. Bañares, A. Trottier, and E. Wrede, J. Chem. Phys. **128**, 014304 (2008).
[33] A. Ichihara and K. Yokohama, J. Chem. Phys. **103**, 2109 (1995).
[34] A. Aguado, O. Roncero, C. Tablero, C. Sanz, and M. Paniagua, J. Chem. Phys. **112**, 1240 (2001).
[35] L. P. Viegas, A. Alijah, and A. J. C. Varandas, J. Chem. Phys. **126**, 074309 (2007).
[36] F. J. Aoiz, V. Sáez Rábanos, T. González-Lezana, and D. E. Manolopoulos, J. Chem. Phys. **126**, 161101 (2007).
[37] F. J. Aoiz, T. González-Lezana, and V. Sáez Rábanos, J. Chem. Phys. **127**, 174109 (2007).
[38] D. Skouteris, J. F. Castillo, and D. E. Manolopoulos, Comput. Phys. Commun. **133**, 128 (2000).
[39] L. Bonnet and J. C. Rayez, Chem. Phys. Lett. **277**, 187 (1997).
[40] L. Bañares, F. J. Aoiz, P. Honvault, B. Bussery-Honvault, and J.-M. Launay, J. Chem. Phys. **118**, 565 (2003).
[41] L. Bonnet and J.-C. Rayez, Chem. Phys. Lett. **397**, 106 (2004).
[42] L. Bonnet, J. Chem. Phys. **128**, 044109 (2008).
[43] E. J. Rackham, F. Huarte-Larrañaga, and D. E. Manolopoulos, Chem. Phys. Lett. **343**, 356 (2001).
[44] E. J. Rackham, T. González-Lezana, and D. E. Manolopoulos, J. Chem. Phys. **119**, 12895 (2003).
[45] M. Quack, Mol. Phys. **34**, 447 (1987).
[46] D. Gerlich, J. Chem. Phys. **92**, 2377 (1990).
[47] K. Park and J. C. Light, J. Chem. Phys. **127**, 224101 (2007).
[48] M. Berbinger and C. Schlier, J. Chem. Phys. **101**, 4750 (1994).
[49] R. S. Dumont and P. Brumer, J. Phys. Chem. **90**, 3509 (1986).